

**TECHNO-ECONOMIC ANALYSIS OF HYBRID PV-BATTERY-DIESEL POWER SYSTEM FOR RURAL ELECTRIFICATION: A CASE STUDY IN IBUDO ORA, OGBOMOSO**

**Abstract**

Fossil-fueled generators and electrical grid extensions are the most popular energy sources for supplying electricity to rural areas. However, the high cost of running and maintenance, noise pollution, and a need for decarbonization necessitate the hybridization of different energy sources as a viable solution. Using the conventional technique for the optimal design of a Hybrid Power System (HPS), such as the Hybrid of Multiple Energy Resources (HOMER), is inefficient regarding electricity cost and carbon emission reduction. Hence, this research conducted a technical and economic analysis of an optimal photovoltaic (PV), battery, and diesel generator-based power system to electrify Ibudo Ora, a rural community in Ogbomoso. A feasibility study on electricity demand was conducted on the Ibudo Ora community by conducting an onsite survey, and the community load profile was estimated. Mathematical modeling of the HPS component was formulated. A multi-objective function was developed to minimize the Net Present Cost (NPC), Levelized Cost of Electricity (LCOE), and Total Carbon Emission (TCE) and maximize the System Reliability (SR) of the proposed HPS and optimized using the Energy Valley Optimizer (EVO). MATLAB R2021a was used to simulate the developed model. The performance of the developed EVO-based HPS was evaluated using NPC, LCOE, TCE, and SR as metrics and compared with HOMER, which was used for the same purpose. The NPC of the developed EVO-based HPS and HOMER-based HPS were \$998702.87 and \$1011984.27, respectively, while the LCOE were \$0.4889 and \$0.4954. The loss of power supply probabilities of the developed EVO-based and HOMER-based HPS was zero, while in terms of TCE, EVO-based HPS and HOMER-based HPS had 775958.15 kg and 832912.49 kg, respectively. The results showed an appreciable reduction in the NPC, LCOE, and TCE using **EVO compared with HOMER for an optimized HPS**. This research will assist the government, investors, and policymakers in making decisions on rural electrification using HPS.

**Keywords:** Hybrid Power System, HOMER, Rural Electrification, Optimization, Energy Valley Optimizer.

**Introduction**

The primary purpose of an electric power system is to give its consumers a sufficient supply of electricity at a reasonable cost and with a high degree of dependability. The need for electricity is perpetually increasing alongside the worsening of global warming caused by the continuous growth in population, urbanization, and rapid industrialization. Consequently, a power generation requirement is proportional to this increase (Nazari-Heris and Mohammadi-Ivatloo, 2018). Traditionally, fossil fuel reserves, including coal, oil, and natural gas, are the primary sources of electricity production. However, these resources have finite reserves, leading to ongoing fuel price increases affecting many nations' economies. The oil shortages in the 1970s spurred considerable interest in energy from renewable sources. Renewable energy is derived from solar

radiation, wind, biomass, water, tides, oceanographic waves, and geothermal heat. The renewable and clean nature of energy sources such as solar, wind, biomass, nuclear fusion, geothermal, and ocean energy has made them highly advantageous as alternative energy sources. Comparing solar energy to other renewable energy sources, it is preferable regarding their availability, affordability, and accessibility, making it one of the best solutions to electricity demand (Kabira et al., 2018; Sawle et al., 2018; Babatunde et al., 2023).

Rural electrification refers to the electricity provision system specifically designed for rural residents. The latest figures from the World Bank Global Electrification Database indicate that 55.4% of the Nigerian populace has access to electrical power. In comparison, only 24.6% of the rural demographic can access it (The World Bank, 2023). Therefore, ensuring an appropriate energy infrastructure for the electrical power supply to rural regions in Nigeria is a pressing concern within the energy industry. While extending the national grid by a power transmission line is often the initial approach for rural electrification, there are instances where this solution is not feasible due to obstacles such as limited transmission networks, difficult terrains, and widely dispersed valleys. Therefore, the off-grid power system provides a quite efficient alternative. A reliable energy supply for remote village areas can be achieved through hybrid power technology (Suresh et al., 2020).

A Hybrid Power System (HPS) is a system that combines two or more means of generating power, either from renewable energy sources or fossil fuel units. HPS is commonly employed in rural and isolated regions. Given that these regions are not connected to the main power system providing them with electricity is expensive and not financially viable. Therefore, dispersed generation is the optimal selection in these areas. Nevertheless, the isolated implementation of distributed generation is not viable as a sustainable solution in the long run because of limited resources and environmental contamination. Dependence on distributed generation as the primary power supply method invariably leads to the yearly release of greenhouse gases.

Furthermore, villages frequently encounter periodic power failures due to their isolated position, scarcity of resources, and high energy expenses. These problems are being addressed, and the intermittent nature of solar and wind resources is being overcome by using HPS to provide electrical energy to this area. A techno-economic analysis is necessary for the hybrid system to effectively use renewable energy resources (Sinha and Chandel 2014; Qi et al., 2022).

Given the high cost of its components, HPS design optimization is crucial. Hence, implementing a less-than-ideal design can substantially impact the long-term economic performance of the HPS. The best size for each HPS component—such as the PV module, battery storage system, diesel generator, and converter—can be chosen by applying optimization approaches to the HPS design (Babatunde et al., 2019; Jumare et al., 2020). The intricacy of the optimal design of hybrid power systems (HPS) has rendered traditional optimization approaches ineffective and inefficient. Over the past twenty years, metaheuristic optimization methods have gained significant popularity. Noteworthy instances of this phenomenon encompass Genetic Algorithm (GA), Firefly Algorithm (FA), Particle Swarm Optimization (PSO), and Cuckoo Search Algorithm (CSA). Metaheuristic optimization methods have several desirable features that make them the preferred option for addressing optimization issues. These advantages encompass their

simplicity, straightforward implementation, and rapid convergence. While a certain metaheuristic algorithm may provide a favorable outcome in a specific scenario, it may exhibit inadequate performance in another one. This motivates scholars to explore new methods to address challenges associated with optimization of HPS (Yahiaouia et al., 2017).

This work aimed to optimize the design of HPS for electrifying Ibudo Ora, a Surulere Local Government Area community in Ogbomoso, Oyo state, Nigeria. The optimal design was achieved using Energy Valley Optimizer (EVO), a new metaheuristic algorithm that draws inspiration from physics principles concerning stability and diverse types of particle decay.

## **Literature Review**

The area of hybrid power systems has caught the attention of many power and energy system researchers; some of their works are reviewed in this section. An overview of applied HPS for global villages, focusing on Malaysia, was presented by Fadaeenejad et al. (2014) to support current and upcoming efforts to improve field performance. They present an appropriate design and analysis for a Malaysian hamlet based on their suggested combination. The results obtained demonstrate that the integration of PV-wind-battery systems is a cost-efficient HPS for communities in Malaysia. In their study to establish the ideal size of a stand-alone HPS for electrifying a remote location in Kerman, Iran, Askarzadeh et al. (2015) adopted particle swarm optimization (PSO). A model was established using three decision variables associated with the system components: the total area occupied by the PV panels, the total swept area by the blades of the rotating turbines, and the number of batteries. The objective function was formulated to minimize the life cycle cost (LCC) and improve system reliability. Their findings demonstrate that the PV/WT/battery system is the most economically efficient model, and the adaptive inertia weight-based PSO algorithm produces more favorable outcomes than other PSO variations. Tito et al. (2016) found that socio-demographic factors determine the optimal size of a stationary wind-PV-battery HPS. A hybrid optimization technique aligned the demand with the existing renewable energy resources. The research findings indicate that the dimensions and configuration of the system are greatly affected by the electrical demand characteristics of a given area.

In 2016, Ogunjuyigbe and Ayodele provided a techno-economic analysis of a stand-alone hybrid energy system for a Nigerian telecom company's base transceiver station. The Homer simulation tool was used to simulate the hybrid energy system in terms of total net present cost (NPC) throughout a selected project lifecycle of 25 years. Their results indicate that the PV/Diesel/Battery configuration has the most favorable cost-benefit ratio among the five economically viable HPS. Furthermore, their findings demonstrated decreased carbon dioxide (CO<sub>2</sub>) and carbon monoxide emissions compared to the non-renewable generating alternative (diesel generator alone).

A study conducted by Yahiaouia et al. (2017) introduced the Grey Wolf Optimizer (GWO), which draws inspiration from the natural leadership rank and hunting strategy observed in grey wolves. Their approach was implemented to reduce the overall expenses of the hybrid power generation system in Djanet, a remote rural community in southern Algeria. A power system that

includes PV, DG, battery banks, and load was examined to evaluate its methodology. The findings achieved by their proposed approach are compared to the PSO algorithm. The findings demonstrate that their proposed methodology efficiently identified the ideal amount of PV panels, DGs, and battery banks, exhibiting rapid convergence and lower cost than PSO.

Movahediyani and Askarzadeh (2018) introduced a multi-objective optimization framework for designing a PV+hydrogen power generation system for a remote village while considering the existence of an operating reserve. Their objective function consisted of total net present cost, CO<sub>2</sub> gas Emission, and loss of power supply probability. The objectives were resolved via a meta-heuristic technique called the Crow search algorithm. Computational simulations demonstrate that including an operating reserve leads to a substantial increase in the system's size (and hence the expense).

Babatunde et al. (2019) analyze the technical, economic, and environmental impacts of an off-grid HPS designed for base stations for transceivers in the Nigerian telecommunications industry. Various performance metrics were utilized to evaluate the feasibility of deploying a hybrid PV-diesel generator and battery system. It was concluded that all BTS sites in the six geopolitical zones in Nigeria could replace the diesel generator (DG) with PV+battery+DG HPS. In addition to the economic benefits compared to distributed generation (DG), HPS designs were reported to exhibit high performance regarding consumption of fuel and emissions of CO<sub>2</sub>.

Krishan and Suhag (2019) provided an economic and technological evaluation of an optimally designed HPS to meet the residential and agricultural electricity demands of an energy-deprived community in the Yamunanagar district of Haryana, India. Three distinct ideal configurations—wind+battery, PV+battery, and wind+PV+battery—were assessed regarding NPC and LCOE to determine the most economically viable option. All necessary modeling and simulation were performed utilizing HOMER software. The results confirmed that a wind/PV/battery-based HPS system is the most economically efficient setup for the site under consideration. It was noted that not all locations, however, have sufficient wind speed to operate the wind turbine.

Qi et al. (2022) examined the implementation of HPS in distant locations, ships, and isles. The cost evaluation of a HPS system was analyzed using the real-life scenario of an aisle in China. The findings indicate that the PV+DG+BSS-based hybrid system, when implemented as an appropriate HPS, can decrease the cost of electricity (COE) by 0.153 \$/kWh and lower the annual CO<sub>2</sub> emissions for the island by 235,945 kg/year. Their validation confirms that HPS with the Battery Storage Systems (BSS) offers notable benefits, such as minimum consumption of fuel and minimum emissions, when equated to HPS without BSS. They also indicate that the PV+Wind+DG+BSS hybrid systems have favorable economic benefits and promising application prospects. However, the financial advantage was considered, disregarding the system's dependability.

Mahmud et al. (2022) utilized HOMER Pro software to develop and optimally design four configurations of HPS with energy storage for Balnasari Qani village, Afghanistan. The location under consideration was situated on a lofty alpine plateau and possessed the capacity to establish off-grid HPS utilizing PV, WT, and biogas. Their work achieved an LCOE of 0.340 \$/kWh and an NPC of \$411,491.

To decrease the overall cost of operation and mitigate emissions, Kamal et al. (2022) devised an approach that integrates renewable energy sources. Their proposed methodology focuses on affordable energy solutions for rural regions in India. The study employed PSO to address the objective problems of minimal cost and emission scenarios. The investigation was conducted on a microgrid consisting of PV, DG, battery, WT, and a load profile representative of an Indian rural environment. Their work demonstrated that adopting an optimized HPS is economically efficient.

Saputra et al. 2024 determined the optimal configuration and sizing of a PV-battery-diesel system for a dockyard in West Papua to minimize CO<sub>2</sub> and LCOE using HOMER software. Also, Mojumder et al. 2024 evaluated the performance of HPS for a remote community using HOMER software. However, the HOMER optimization approach is straightforward and does not thoroughly optimize the HPS. Furthermore, Some of its drawbacks are the lengthy calculation times and inability to perform multi-objective optimization of the HOMER software (which solely aims to minimize the NPC) (Hoarcă et al., 2023).

From the literature reviewed, it was observed that many works have been proposed for the optimal configuration of HPS, and different components have been combined using various algorithms. However, due to the need for better and more accurate performance in optimizing the components of HPS, it is therefore necessary to develop a new method for their optimization. Hence, EVO is proposed. When tested on real-world problems, the EVO optimizer's performances revealed that it could give exceptional and competitive outcomes in addressing intricate benchmarks and real-world scenarios (Azizi et al., 2023).

Also, from the literature reviewed, it was discovered that the outcome of HPS varies with the location of consideration, and optimal HPS has not been designed for the proposed site for rural electrification purposes before now. These make the proposed HPS unique and promising.

## **Methodology**

### **Site Description and Data Collection**

The primary aim of rural electrification is to facilitate the electrification of the communities or settlements not connected to the national grid. Ibudoora is a community in Ogbomosho that is currently not connected to the national grid. Apart from not being connected to the grid, this village is proposed due to its structure. The buildings are compact, with very few scattered. Visitation was made to this village for a feasibility study, and an energy demand estimation was carried out. To analyze this proposed hybrid system, the meteorological data of solar irradiance, clearness index, and temperature of the proposed site were collected from the National Aeronautics and Space Administration (NASA) through their website ([www.power.larc.nasa.gov](http://www.power.larc.nasa.gov)).

### **System Modelling**

The essential components responsible for the performance of the proposed HPS are solar PV, DG set, battery storage system, and the power converter. The focus was made on the output power of these components. An essential first step in HPS size optimization is modeling these components. It is a crucial tool that shows how well system components operate in different scenarios (Suresh

et al. 2020). The following subsections describe the mathematical modeling of the suggested HPS components.

### Mathematical modeling of PV system

In a PV system, there are several PV modules. As depicted in Fig. 1(a), the PV module with a single diode is considered. Short and open circuits are equivalent to low series and large shunt resistance. Fig. 1(b) illustrates a simplified circuit of a photo voltaic module. The PV system was modeled as given by Chauhan and Saini (2016). Using Equation 3.1, the voltage of a PV module ( $V_{PV}$ ) is determined using Equation 1:

$$V_{PV}(t) = V_{mp} \left[ 1 + 0.0539 \log \left( \frac{E_u(t)}{E_{st}} \right) \right] + \alpha(T_a(t)) + 0.02E_u(t) \quad 1$$

In this context,  $V_{mp}$  represents the module voltage at maximum power in volts (V),  $\alpha$  denotes the temperature component of the open-circuit voltage,  $E_u$  signifies solar radiation in kW/m<sup>2</sup>,  $E_{st}$  refers to standard solar radiation (1 kW/m<sup>2</sup>), and  $T_a$  indicates ambient temperature (in K).

The photo-current ( $I_{ph}$ ) of a PV module is contingent upon the incident solar energy and temperature, and may be computed using Equation 2, as follows:

$$I_{ph}(t) = [I_{sc} + \beta(T_a(t) - T_r)] * \frac{E_u(t)}{E_{st}} \quad 2$$

where  $T_r$  is the reference temperature (in Kelvin),  $I_{sc}$  is the short circuit current of the PV module in Amperes (A), and  $\beta$  is the temperature coefficient of the short circuit current of the PV module. Using Equation 3, the PV module saturation current ( $I_{rs}$ ), this is temperature-dependent and may be computed using Equation 3, expressed as:

$$I_{rs}(t) = I_{rr} \left( \frac{T_a(t)}{T_r} \right)^3 \exp \left[ \frac{qE_g}{KA_i} \left( \frac{1}{T_r} - \frac{1}{T_a(t)} \right) \right] \quad 3$$

where  $I_{rr}$  is the reverse saturated current of the solar module,  $q$  represents the electron charge,  $K$  denotes Boltzmann's constant,  $A_i$  is the ideality factor of PV module and  $E_g$  is band gap energy.

The current output of PV module ( $I_{pv}$ ) was calculated according to Equation 4, given as:

$$I_{pv}(t) = I_{ph}(t) - I_{rs}(t) \left[ \exp \left( \frac{qV_{PV}(t)}{N_s K T_a(t) A_i} \right) - 1 \right] \quad 4$$

where,  $N_s$  is number of cells in PV module. At any hour  $t$ , power output of a solar PV system ( $P_{PV\_OUT}$ ) in Watt is expressed as:

$$P_{PV\_OUT} = N_{PV} * V_{PV}(t) * I_{PV}(t) \quad 5$$

where,  $N_{PV}$  is number of PV modules.

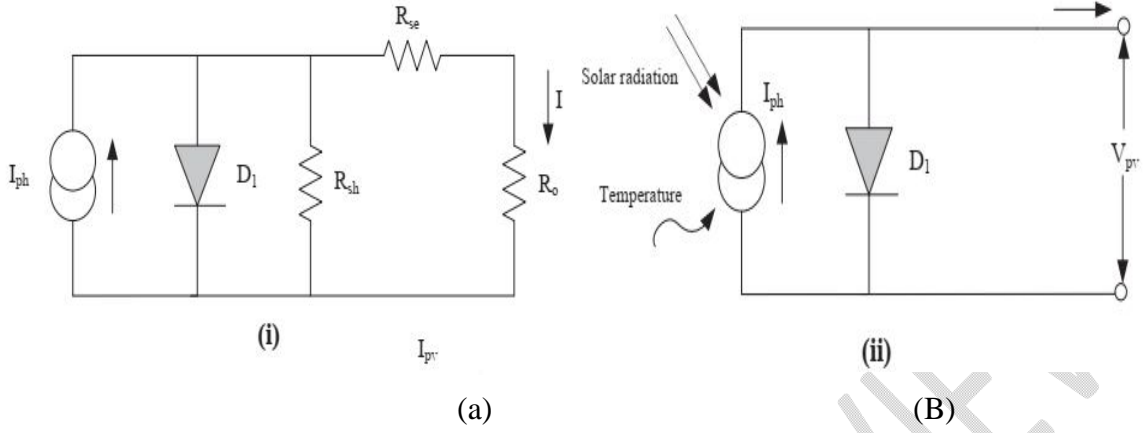


Fig. 1: Single diode model of PV modules (i) equivalent circuit (ii) simplified circuit

(Source: Chauhan and Saini 2016)

### Battery Storage modelling

The needed capacity for storage of the battery system in Ampere-hours (Ah) was calculated using Equation 5, given as (Ogunjuyigbe *et al.* 2016):

$$M_{bat} = \frac{A_d * E_L}{\eta_{bat} * \eta_{inv} * DoD * V_s} \quad 5$$

In this context,  $A_d$  represents the battery's autonomous days, indicating the maximum duration the battery can provide continuous energy without recharging from any power source.  $E_L$  denotes the total energy demand from the storage system,  $DoD$  signifies the maximum allowable depth of discharge of the battery, and  $V_s$  refers to the system voltage measured in volts.

Battery storage systems were produced in nominal capacities ( $C_B$ ). This denotes the battery storage's maximum charge capacity. The state of charge,  $soc(t)$ , of the battery at any time  $t$  represents the battery's charge quantity at that specific moment. It is constrained by  $Soc_{min}$  and  $Soc_{max}$  as follows:

$$SOC_{min} \leq SOC(t) \leq SOC_{max} \quad 6$$

where  $SOC_{min}$  is the minimum charge quantity of the battery storage while  $SOC_{max}$  is the maximum charge quantity of the battery storage.  $SOC_{min}$  is dependent on the depth of discharge ( $DoD$ ). This can be expressed as:

where  $SOC_{\min}$  represents the minimum charge capacity of the battery storage, and the maximum charge capacity of the battery storage is denoted as  $SOC_{\max}$ .  $SOC_{\min}$  is contingent upon the  $DoD$  of the battery. This may be formulated as:

$$SOC_{\min} = (1 - DoD) * C_B \quad 7$$

At maximum charge, state of charge is expressed as:

$$SOC(t) = SOC_{\max} = C_B \quad 8$$

### Diesel Generator modelling

The diesel generator serves as a supplementary energy source, operating solely when required. The diesel generator's output power was determined using Equation 9, as presented by Kharrich et al. (2021):

$$E_{DG} = \frac{F(t) - A_g \times P_r}{B_g} \quad 9$$

where  $F$  the fuel consumption,  $P_r$  is the rated electric power of Diesel generator (kW),  $A_g$  and  $B_g$  are constants of the linear consumption of the fuel.

The fuel consumption ( $F$ ), and  $CO_2$  emission ( $E_{CO_2}$ ) of a generator are measured each time it is turned on. Each time the generator is turn on, generator's hours-of-run,  $H$ , is likewise increased. The hours-of-run are used to calculate the runtime or consumption of the generator and to predict when maintenance and replacement are required.

The amount of fuel used in liters per hour of a generator at time  $t$  is correlated with the nominal power of the diesel generator and the actual electrical output of this diesel generator, as expressed in Equation 10 (Ogunjuyigbe et al., 2016):

$$F(t) = \left( 0.246 \times \frac{E_{x/d}(t)}{1h} \right) + (0.08415 \times P_r) \quad 10$$

where 0.246 is an empirical factor in l/kWh, and 0.08415 is also an empirical factor in l/kWh. The total fuel consumption for a generator throughout the lifecycle of the system is the sum of all hourly fuel consumptions is given using Equation 3.11, given as:

$$F_{gen} = \sum_{t=1}^n F(t) \quad 11$$

Similar to this, the  $CO_2$  emission and associated hours of run for generators 1, 2, and 3 are provided as follows:

$$E_{co_2}(t) = S_{E(CO_2)}(kg/l) \times F(t)(l/h) \quad 12$$

where is  $S_{E(CO_2)}$  the specific emission of carbon dioxide per liter of fuel and it is given as 2.7 kg/l. The  $CO_2$  emission of a generator throughout the lifecycle of the system ( $E_{co_2total}$ ), is the sum of all hourly  $CO_2$  emissions. This is given as:

where  $S_{E(CO_2)}$  represents the particular emission of gases such as CO<sub>2</sub> per liter of fuel, quantified as 2.7 kg/l. The carbon footprint of a generator over its lifecycle ( $E_{co_2total}$ ) are the aggregate of all hourly emissions of CO<sub>2</sub>. This is provided as follows:

$$E_{co_2total} = \sum_{t=1}^n E_{co_2}(t) \quad 13$$

## Problem Formulation

This study aimed to design a hybrid power system using energy valley optimizer (EVO) for rural electrification. To achieve this, a multi-objective optimization model was formulated to minimize the net present cost (NPC), levelized cost of electricity (LCOE), system reliability (SR) and total carbon emission ( $E_{co_2total}$ ) of the developed HPS. This was formulated using Equation 14, given as:

$$Fitness = minimize(NPC, LCOE, SR, EM_{co_2total}) \quad 14$$

### 3.5.1 Net present cost

The total of the capital expenses and the system's discounted future expenditures over the course of the project's lifetime is known as the net present cost. The total NPC encompasses initial capital expenditures, replacement expenditures, maintenance expenditures, and fuel expenditures. Consequently, the reduction of the NPC of the proposed HPS is addressed using Equation 15, given as (Chauhan and Saini 2016; Suresh et al., 2020; Jumare et al., 2020):

$$NPC = minimize\left(\frac{TAC}{R}\right) \quad 15$$

where TAC denotes the total annualized cost of the system and R represents the capital recovery factor. The capital recovery factor (R) of a component or system is dependent on the annual real interest rate (r) and the usable lifespan of the component or system (n), and is computed using Equation 16, expressed as:

$$R = \frac{r(1+r)^n}{(1+r)^n - 1} \quad 16$$

$$TAC = AC_C + AC_{O\&M} + AC_{REPL} + AC_F \quad 17$$

where  $AC_C$  is annualized capital cost,  $AC_{O\&M}$  is annualized operation and maintenance cost,  $AC_{REPL}$  is annualized replacement cost and  $AC_F$  is annualized fuel cost. Annualized capital cost of HPS is the sum of the capital costs of different system components and can be estimated using Equation 18:

Where  $AC_C$  represents the annualized capital cost,  $AC_{O\&M}$  denotes the annualized operation and maintenance cost,  $AC_{REPL}$  signifies the annualized replacement cost, and  $AC_F$  indicates the annualized fuel cost. The  $AC_C$  of HPS is the aggregate of the capital costs of various system components and may be calculated using Equation 18:

$$AC_C = AC_{C_{PV}} + AC_{C_{DG}} + AC_{C_{BSS}} + AC_{C_{CONV}} \quad 18$$

where  $AC_{C_{PV}}$  is the annualized capital cost of PV,  $AC_{C_{DG}}$  is the annualized capital cost of DGs,  $AC_{C_{BSS}}$  is the annualized capital cost of battery and  $AC_{C_{CONV}}$  is the annualized capital cost of power converter.

Annualized capital cost of PV ( $AC_{C_{PV}}$ ) was estimated according to Equation 19, given as:

$$AC_{C_{PV}} = R_{PV} \times [N_{PV} \times (C_{PV} + C_{IN_{PV}})] \quad 19$$

where  $R_{PV}$  is  $R$  of PV module,  $N_{PV}$  is the number of PV module needed,  $C_{PV}$  is initial capital cost of a PV module (\$) and  $C_{IN_{PV}}$  is the cost of installing a PV module (\$).

Annualized capital cost of DGs ( $AC_{C_{DG}}$ ) was estimated according to Equation 20, given as:

$$AC_{C_{DG}} = R_{DG} \times (Ng \times P_{dg}) C_{DG} \quad 20$$

where  $R_{DG}$  is  $R$  of DG,  $Ng$  is the number of split DG needed,  $P_{dg}$  is the DG rating in kW and  $C_{DG}$  is the capital cost per kW.

Annualized capital cost of battery ( $AC_{C_{BSS}}$ ) was calculated according to Equation 21, given as:

$$AC_{C_{BSS}} = R_{BSS} \times (N_{BSS} \times C_{BSS}) \quad 21$$

where  $R_{BSS}$  is capital recovery factor of battery,  $N_{BSS}$  is the number of Battery module needed and  $C_{BSS}$  is initial capital cost of a Battery (\$)

Annualized capital cost of power converter ( $AC_{C_{CONV}}$ ) was estimated according to Equation 22, given as:

$$AC_{C_{CONV}} = R_{CONV} \times P_{INV} \times C_{CONV} \quad 22$$

where  $R_{CONV}$  is  $R$  of the power converter,  $P_{INV}$  is the converter power input,  $C_{CONV}$  is the initial cost of the power converter in \$/kW.

Annualized operation and maintenance cost ( $AC_{O\&M}$ ) of the proposed system was calculated according to Equation 23, given as (Kharrichet *al.* 2021):

$$AC_{O\&M} = AC_{O\&M_{PV}} + AC_{O\&M_{BSS}} + AC_{O\&M_{DG}} + AC_{O\&M_{CONV}} \quad 23$$

$$AC_{O\&M_{PV}} = C_{AOM_{PV}} \times N_{PV} \times \sum_{i=1}^n \left( \frac{1+\mu}{1+r} \right)^i \quad 24$$

$$AC_{O\&M_{BSS}} = C_{AOM_{BSS}} \times N_{BSS} \times \sum_{i=1}^{n_{BSS}} \left( \frac{1+\mu}{1+\delta} \right)^{(i-1)L_{BSS}} \quad 25$$

$$AC_{O\&M_{DG}} = (C_{AOM_{DG}} \times N_{DG_{min}}) \times \sum_{i=1}^n \left( \frac{1+\mu}{1+r} \right)^i \quad 26$$

$$AC_{O\&M_{CONV}} = C_{AOM_{CONV}} \times \sum_{i=1}^n \left( \frac{1+\mu}{1+r} \right)^i \quad 27$$

where  $\mu$  is escalation rate (%)  $\delta$  is inflation rate (%),  $L_{BSS}$  is battery life cycle,  $C_{AOM_{PV}}$ ,  $C_{AOM_{BSS}}$ ,  $C_{AOM_{DG}}$  and  $C_{AOM_{conv}}$  are the annual operation & maintenance cost of the PV, battery, diesel generators and power converter respectively.

Furthermore, annualized replacement cost ( $AC_{REPL}$ ) was estimated according to Equation 28, given as (Ogunjuyigbe *et al.* 2016):

$$AC_{REPL} = C_{DG,BSS} \times C_{Nom} \times \sum_{i=1}^{N_{REPL}} \left[ \frac{1+\delta}{1+r} \right]^{\frac{N}{N_{REPL}+1}} \quad 28$$

where  $C_{Nom}$  is the nominal capacity (W) of the replacement and  $N_{REPL}$  is the number of times the component is replaced over the systems lifecycle. The replacement cost of other component is not considered because their lifecycle is within the project life span.

Annualized fuel cost ( $AC_F$ ) can be calculated as:

$$AC_F = F_{cost/liter} \times F_{system} \quad 29$$

where  $F_{cost/liter}$  is the cost of Diesel per liter.

### 3.5.2 Levelized cost of electricity

The levelized cost of electricity (LCOE) represents the average cost per kilowatt-hour of useful electrical energy produced by the system. The LCOE for the generation of the proposed Hydro Pumped Storage (HPS) can be calculated as (Chauhan and Saini 2016):

$$LCOE = minimize \left( \frac{TAC}{E_{Demand}} \right) \quad 30$$

where  $E_{Demand}$  is the yearly electrical power consumption of the research area (kWh/yr).

### 3.5.3 System reliability

System reliability was measured using the loss of power supply probability, or LPSP. LPSP is defined as the likelihood that an inadequate power supply occurs when HPS fails to meet the electrical power requirement. The reliability of the system in meeting the load was achieved by minimizing the value of LPSP which can be calculated according to Equation 31, given as (Chauhan and Saini 2016):

$$SR = minimize(LPSP) \quad 31$$

$$LPSP = \frac{\sum_{t=1}^{8760} LPS(t)}{\sum_{t=1}^{8760} E_{Demand}(t)} \quad 32$$

where  $LPS$  is loss of power supply at hour 't' was estimated using equation 3.33 as:

$$LPS(t) = E_{Demand}(t) - [E_{PV}(t) + E_{BSS}(t) + E_{DG}(t)] \times \eta_{INV}$$

33

where  $E_{PV}(t), E_{BSS}(t), E_{DG}(t)$  is the energy supplied by PV, Battery, and DGs respectively.  $\eta_{INV}$  is power converter efficiency.

### 3.5.4 Total carbon emission

The cumulative CO2 emissions of the system over its entire lifecycle constitute the aggregate of the total CO2 produced by the generator. This can be calculated according to Equation 34, given as:

$$EM_{co_2total} = minimize (E_{co_2total_{DG}}) \quad 34$$

### 3.6 Operational Constraints

The formulated objective function for this study is optimized under the constraints which are discussed follows (Chauhan and Saini 2016):

#### 1) Upper and lower bounds

The dimensions of the PV, DGs, and battery storage have been adjusted to satisfy the electrical energy requirements of the research region. The upper and lower limits for these components are expressed as follows:

$$0 \leq N_{PV} \leq N_{PV}^{max} \quad 35$$

$$0 \leq N_{DG} \leq N_{DG}^{max} \quad 36$$

$$0 \leq N_{BSS} \leq N_{BSS}^{max} \quad 37$$

$$N_{PV}, N_{DG}, N_{BSS} = Integer \quad 38$$

where  $N_{PV}^{max}$  is maximum number of PV needed,  $N_{DG}^{max}$  is the maximum number DGs needed and  $N_{BSS}^{max}$  is maximum number of batteries needed.

#### 2) Constraint of battery bank storage limits

Battery bank must not be overcharged or over-discharged at any time t. As a result, the battery bank has been subject to the following restrictions to run within safe limits:

$$E_{BSS_{min}} \leq E_{BSS}(t) \leq E_{BSS_{max}} \quad 39$$

#### 3) Land use constraints for the installation of PV modules

The total land availability ( $LA_{site}$ ) for installing PV modules must be considered as it plays a significant role in determining the number of sizes that can be installed within a given area of land. Therefore, the total area of land required for the installation of PV system ( $LR_{PV}$ ) is subjected to the following constraint according to Equation 40, given as:

$$LR_{PV} \leq LA_{site} \quad 40$$

#### 4) Power generation constraints

The total energy output of the system ( $E_{Total}$ ) at time  $t$  is subjected to the following constraint:

$$E_{Total}(t) > E_{Demand}(t) \quad 41$$

where  $E_{Total}$  is expressed according to Equation 3.42, given as:

$$E_{Total}(t) = N_{PV} \times E_{PV}(t) + N_{DG} \times E_{DG}(t) + N_{BSS} \times E_{BSS}(t) \quad 42$$

### Operation Strategy of the Proposed Hybrid PowerSystem

Fig.2 depicts the operation of the proposed HPS. The operational strategy of the proposed HPS is summarized as follows:

- i. When the battery is fully charged and the load demand ( $E_{Demand}(t) / \eta_{INV}$ ) is less than the total power generated by solar panels ( $E_{PV}(t)$ ), the battery banks are charged to the capacity of the inverter, and any excess power is dumped.

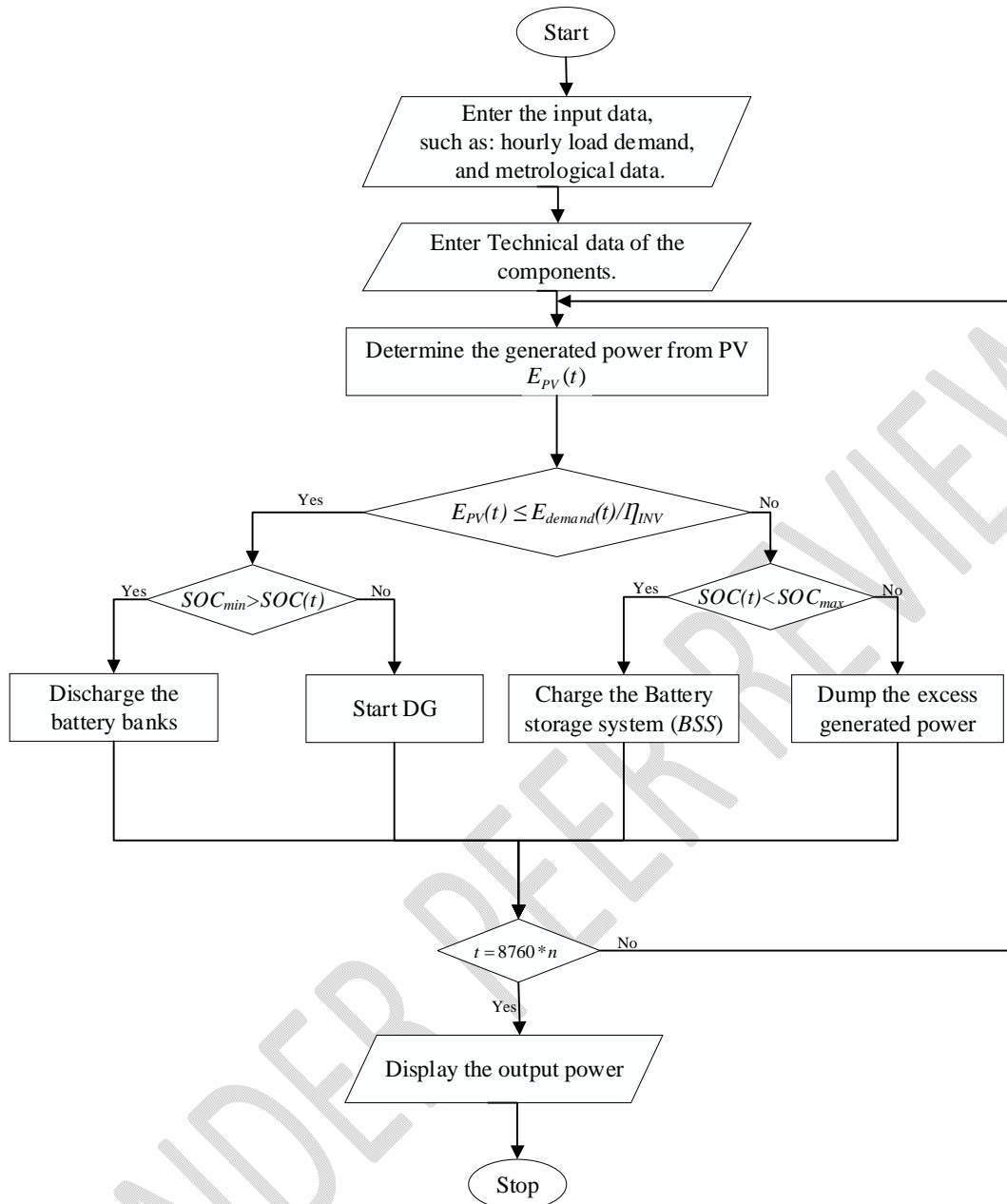


Fig. 2: Operation Strategy of the Proposed HPS

- i. If the battery  $SOC(t)$  is less than  $SOC_{\max}(t)$ , the excess power is used to charge the battery.
- ii. The banks of the battery will supply the insufficiency's power if the load demand ( $E_{Demand}(t) / \eta_{INV}$ ) is larger than  $E_{PV}(t)$  and  $SOC(t)$  of the battery banks is greater than  $SOC_{\min}(t)$ . Otherwise, DGs are activated to meet the load demand and for charging the battery banks if  $SOC(t)$  of the battery banks is less than  $SOC_{\min}(t)$ .
- iii. The operation of DGs depends on the size of load demand at an instant of time.

### **Energy Valley Optimization Algorithm**

The Energy Valley Optimizer (EVO), introduced by Azizi et al. in 2023, is a revolutionary metaheuristic algorithm derived from sophisticated physics concepts related to stability and various forms of particle disintegration.

#### **Inspiration of EVO**

The stability of particles is defined as an energy valley based on binding energies and interactions with other particles. Experts have successfully discerned valuable patterns to elucidate particle disintegration via firsthand observation of diverse phenomena. A particle with a lower energy level is created during the decay process, whereas too much energy is released. The decay process in particles with various levels of stability is controlled by three main types of emissions. The dense, positively charged particles identical to helium are known as alpha particles ( $\alpha$ ). The negatively charged beta ( $\beta$ ) particles are described as electrons moving more quickly, while Gamma ( $\gamma$ ) rays represent higher energy photons. This method utilizes the propensity of particles to attain a stable position as a source of inspiration to improve the efficacy of solution options (Azizi et al., 2023).

#### **Application of EVO for HPS**

The number of solar panels (PV), DGs, and batteries were taken as the decision variables for the proposed method. Fig. 3 presents the flowchart of the proposed method. The following are the procedural steps that were taken in applying EVO algorithm to solve the problem of sizing the components of hybrid power system.

Step 1: Enter the input data. In this step, the input data are defined including the costs of investment, maintenance and replacement of hybrid system components, the data related to the load demand, solar insolation and temperature in the studied area, the population size and the maximum number of iterations.

Step2: Generate the initial positions of the solution candidates ( $X_i$ ) as particles in the searchspace using Equation 43 and 44

$$X = \begin{bmatrix} X_1 \\ X_2 \\ \vdots \\ X_i \\ \vdots \\ X_n \end{bmatrix} = \begin{bmatrix} x_1^1 & x_1^2 & \dots & x_1^j & \dots & x_1^d \\ x_2^1 & x_2^2 & \dots & x_2^j & \dots & x_2^d \\ \vdots & \vdots & \vdots & \vdots & \vdots & \vdots \\ x_i^1 & x_i^2 & \dots & x_i^j & \dots & x_i^d \\ \vdots & \vdots & \vdots & \vdots & \vdots & \vdots \\ x_n^1 & x_n^2 & \dots & x_n^j & \dots & x_n^d \end{bmatrix}, \begin{cases} i = 1, 2, \dots, n. \\ j = 1, 2, \dots, d. \end{cases} \quad 43$$

$$x_i^j = x_{i,min}^j + rand(x_{i,max}^j - x_{i,min}^j), \begin{cases} i = 1, 2, \dots, n. \\ j = 1, 2, \dots, d. \end{cases} \quad 44$$

where n is the total number of particles (solution candidates) in the universe (search space); d is the dimension of the considered problem;  $x_i^j$  is the  $j^{\text{th}}$  decision variable for determining the initial position of the  $i^{\text{th}}$  candidate;  $x_{i,min}^j$  and  $x_{i,max}^j$  represent the lower and upper bounds of the  $j^{\text{th}}$  variable in the  $i^{\text{th}}$  candidate; rand is a uniformly distributed random number in the range of [0, 1].

where n denote the overall number of particles (solution candidates) within the entire universe (search space); d signifies the size of the problem under consideration;  $x_i^j$  represents the  $j^{\text{th}}$  choice variable used to ascertain the starting location of the  $i^{\text{th}}$  candidate;  $x_{i,min}^j$  and  $x_{i,max}^j$  indicate the lower and upper limits of the  $j^{\text{th}}$  variable for the  $i^{\text{th}}$  candidate; rand is a random number that is evenly distributed within the interval [0, 1].

Step3: Evaluate the fitness values for initial solution candidates as Neutron Enrichment Level ( $NEL_i$ ) using Equation 14 and evaluate the problem constraints. Should the problem constraints be unmet, the associated objective function incurs a penalty.

Step4: Estimate the Enrichment Bound ( $EB$ ) of the particles using:

$$EB = \frac{\sum_{i=1}^n NEL_i}{n}, i = 1, 2, \dots, n. \quad 45$$

Step5: Determine the stability levels ( $SL_i$ ) of the particles are determined as follows based on the objective function evaluations:

$$SL_i = \frac{NEL_i - BS}{WS - BS}, i = 1, 2, \dots, n. \quad 44$$

Step6: If the stability level ( $SL_i$ ) is lesser than stability bound ( $SB$ ), Generate alpha index I and II to get the new position vectors using equation 3.45 and go to Step7. Else, determine the center of particles ( $X_{cp}$ ) of the particles using equation 3.46 and go to Step8.:

$$X_i^{New1} = X_i \left( X_{BS}(X_i^j) \right), \begin{cases} i = 1, 2, \dots, n. \\ j = \text{Alpha Index II}. \end{cases} \quad 45$$

$$X_i^{New1} = X_i + \frac{r_1 * X_{BS} - r_2 * X_{CP}}{SL_i}, i = 1, 2, \dots, n. \quad 46$$

Step7: Determine the neighboring particle by generating the gamma index I and II using equation 3.47 and go to Step9.:

$$X_i^{New2} = X_i \left( X_{Ng} (X_i^j) \right), \begin{cases} i = 1, 2, \dots, n. \\ j = \text{Gamma Index II.} \end{cases} \quad 47$$

Step8: Determine the neighboring particle using equation 3.48 and go to Step9.:

$$X_i^{New2} = X_i + (r_3 * X_{BS} - r_4 * X_{Ng}), i = 1, 2, \dots, n. \quad 48$$

Step9: Return the particle stability level ( $X_{BS}$ ). Repeat Step3 to Step9 if the number of functions evaluated is less than the maximum number of iterations (Function evaluation), else go to Step10.

Step10: Stop

UNDER PEER REVIEW

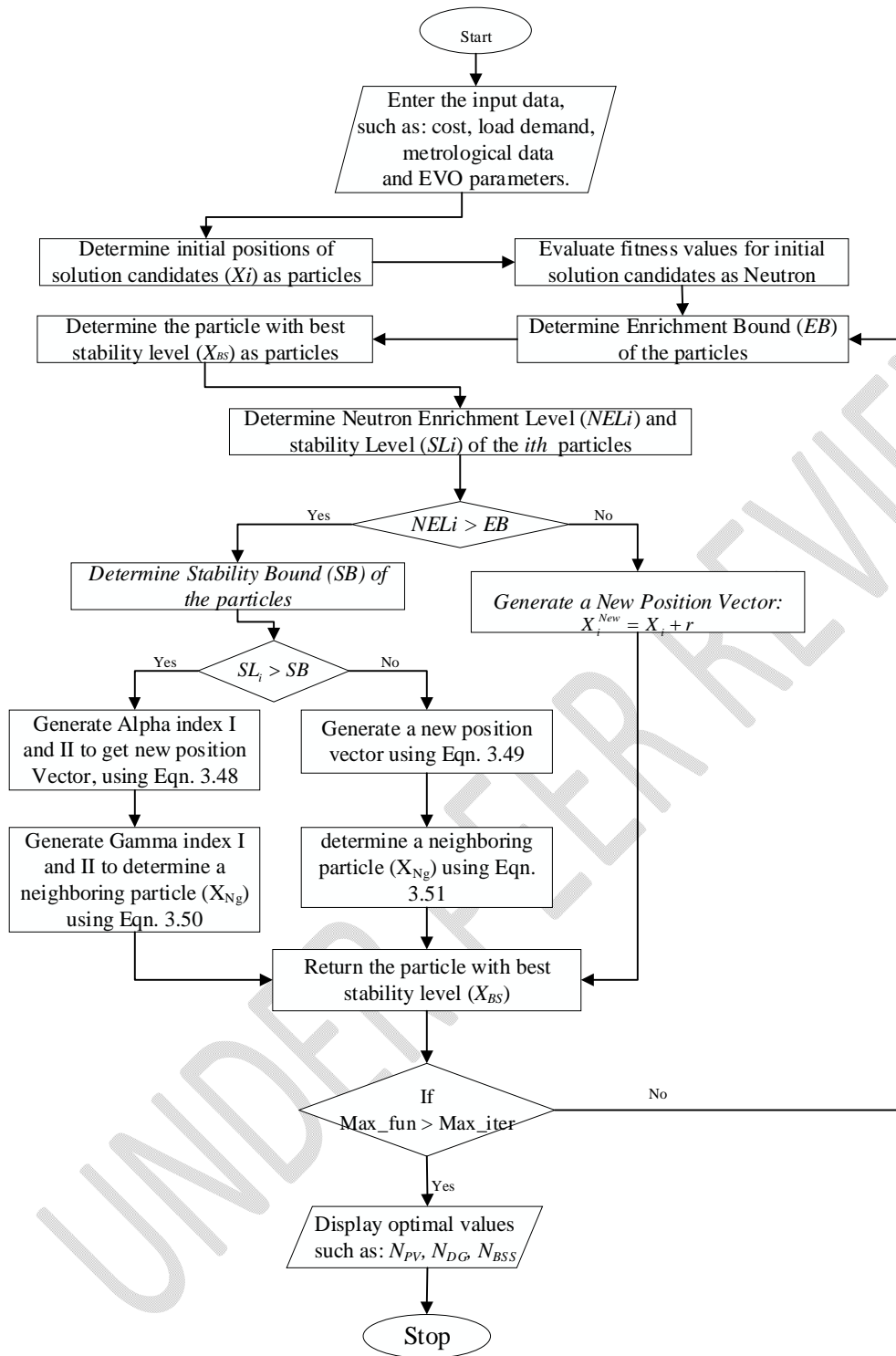


Fig. 3: The Flowchart of the HPS Optimization using EVO

## Results and Discussion

### Feasibility Study

The regional view of the proposed site on the map is presented in Fig 4. The proposed location's latitude and longitude are 8.0723N and 4.4149E, respectively. From the load evaluation carried out, the total load demand of the community is 271.7kW per day, with peak load demand of 19.3kW at 8 am and 8 pm. The hourly load profile is presented in Fig. 5. From Fig. 5, it can be deduced that the

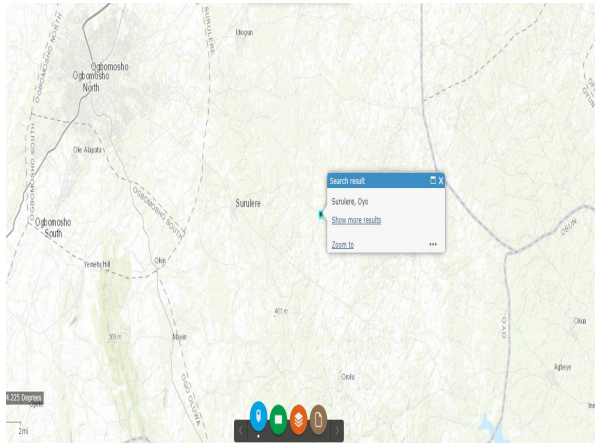


Fig. 4: The Regional View of the Proposed Site

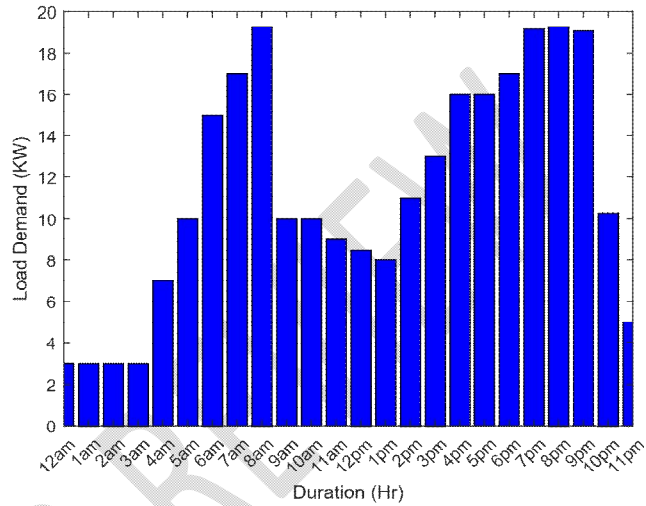


Fig. 5: Hourly Load Profile

peak load demand was recorded around 8 am and 8 pm due to the nature of the villagers' occupation, mainly farming. The farmers leave home in the morning and return in the evening. The solar irradiance, clearness index, and the temperature of the site were collected to evaluate the feasibility of using solar energy, and the results were presented in Fig. 6, 7, and 8. The average daily irradiance data is 5.609 kW/m<sup>2</sup>, the clearness index is 0.7, and the peak temperature is 30.08 °C. The value of the clearness index implies that the weather is clear by 70%; this shows that solar PV will be appropriate there since there is a direct proportionality between the clearness index and solar irradiance that PV panel can absorb. PV power production is always poor in cloudy weather; hence, it needs clear weather to attain its peak production. The average daily clearness index, solar irradiance, and temperature reveal that the usage of solar energy in the proposed site is feasible as the value of irradiance and clearness index are remarkably high, with a moderate temperature (slightly above 25°C STC of most solar PV).

### Simulation Results of HPS Components

The main components of HPS, such as solar PV, battery storage, Diesel Generator (DG), and power converter, were modeled and combined to form the entire system. Each unit is modeled as proposed in the methodology section of this study. The output of a single solar PV for 24 hours is presented in Fig. 9. The total generated power per day is 2.38kW. It can be

observed that between 12am-7 am and 7 pm-12am, the output power from the PV unit is zero (0). The output of the PV rises from 7am and falls back at 7 pm while the peak power output is recorded around 1pm. This validates the intermittent nature of the PV as its production depends on the weather conditions. The state of charge of the battery increases when the battery is charging. At the same time, it decreases when the battery discharges (This is described in Fig. 12). The DG unit was designed to supply the load demand when the PV's generated power is insufficient. The battery charge's state is below the minimum (i.e., less than 20%). The operation of the power converter depends on the power supplied and drawn from it; it acts as the interface between the DC bus and the AC bus.

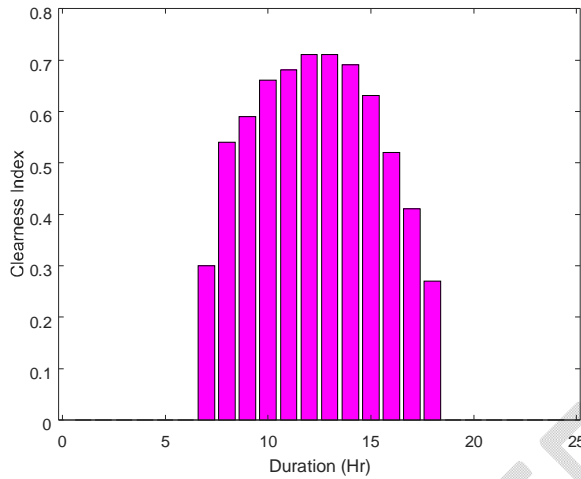


Fig. 6: Hourly Solar Irradiance

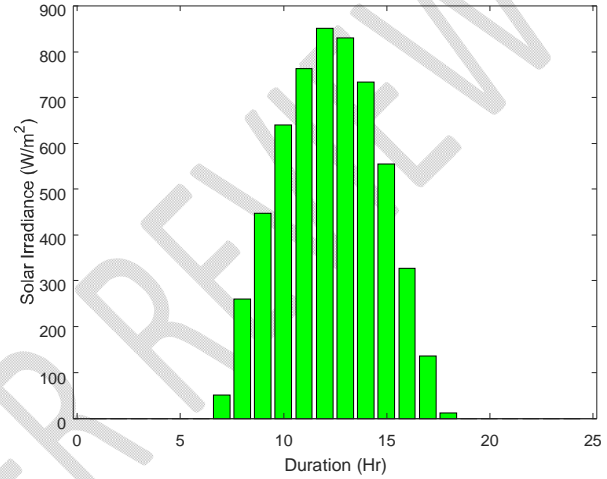


Fig. 7: Hourly Clearness Index

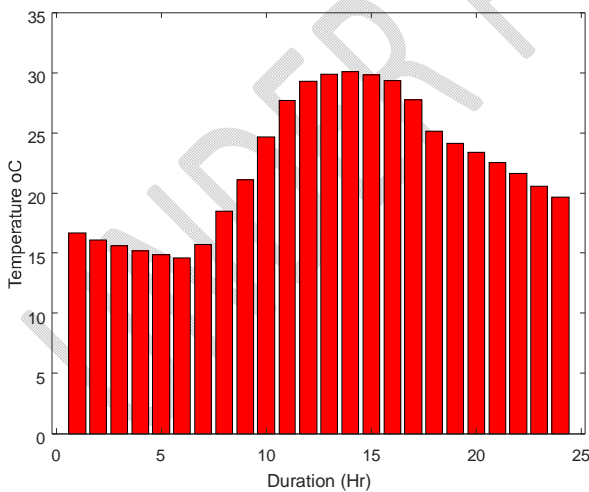


Fig. 8: Hourly Temperature

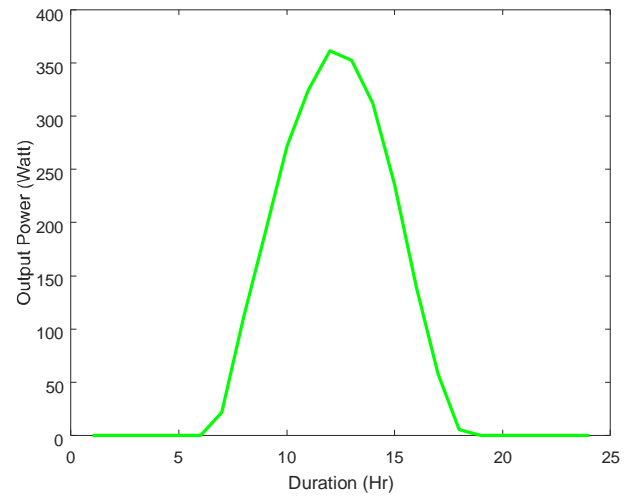


Fig. 9: Hourly Generated Power of a Single PV Panel

**Optimal Sizing of HPS Components using EVO**

The components of the HPS were optimally sized to meet the energy demand of the proposed site using the proposed EVO. The objectives are to minimize the NPC, LCOE, and TCE and maximize system reliability. To analyze the techno-economic benefits of the proposed methodology, three cases were considered, these are:

- i. Case 1: DG only
- ii. Case 2: Only PV and Battery
- iii. Case 3: EVO-optimized HPS

The simulation results of these cases are presented and discussed in the sub-section 4.4.1-4.4.3.

### Case 1: DG Only

The conventional way of generating off-grid electricity is DG. DG was used in this work to serve as the base case for evaluating the performance of the proposed EVO-based HPS. The simulation results are presented in Table 1. The rating of the DG needed to meet the load demand of the community was estimated to be 22kW. The system's capital cost is \$ 11000, while the NPC of the system after 20 years is \$ 1676457.41. The cost of electricity per kWhr for this case was 0.8206.

Regarding system reliability, the Loss of Power Supply Probability (LPSP) is 0.00, which implies that the system under this operation had all the load demands met with 100% reliability. The total CO<sub>2</sub> emission for 20 years of operation is 2074176.57 kg; this implies that 11.83kg of carbon emission is released per hour for 20 years. The system behavior for the period of 48hrs is presented in Fig. 10. From Fig. 10, the output power of the DG followed the pattern load profile, which implies that there is precise control over the output power of the DG.

Table 1: Simulation Result for all the Cases Considered

Parameter	Case 1	Case 2	Case 3
Number of PV Panel	-	22kW	208
Number of Battery Unit	-	175200	45
DG Rating	22kW	-	22.00kW
Hours of operation of DG	175200	-	80200
Capital Cost	\$ 11000	\$ 909450	\$ 326000.00
Replacement Cost	\$ 135350.81	\$ 798590.62	\$ 193731.16
Operation and Maintenance cost	\$ 140987.31	\$ 193133.30	\$ 114285.17
Fuel Cost	\$ 1404996.39	-	\$ 525615.04
Salvage cost	\$ 15877.10	\$ 611196.32	\$ 160928.50
NPC	\$ 1676457.41	\$ 1289977.60	\$ 998702.87
LCOE	0.8206 \$/kWhr	0.6314 \$/kWhr	0.4889 \$/kWhr
LPSP	0.00	0.0817	0.00
TCE	2074176.57 kg	0.00kg	775958.15 kg

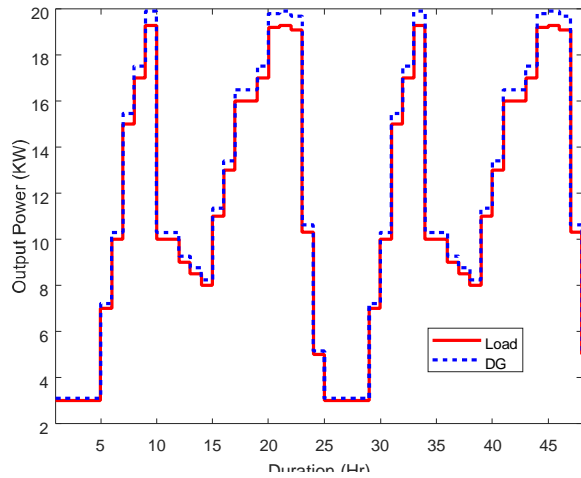


Fig. 10: System Behavior for 48hrs for Case 1.

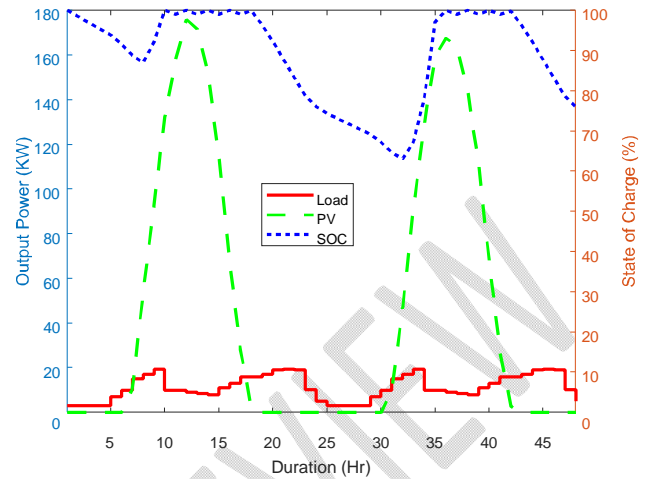


Fig. 11: System Behavior for 48hrs for Case 2

### Case 2: Only PV and Battery

Solar PV and battery storage were used to supply the electricity demand of the proposed community, and this scenario was considered as Case 2. The simulation results for this case are presented in Table 1. In this scenario, 486 modules of 500watt panels are required, along with 248 units of 250AH batteries, to supply the load demand of the proposed community. The system's capital cost is \$ 909450, while the NPC for 20 years of operation is \$ 1289977.60. The cost of electricity per kWhr under this operation is 0.6314 \$/kWhr. The LPSP recorded for this case is 0.0821; this implies that the system can fail to meet the load demand, though not often; hence, the system's reliability is 91.79%. In this case, the TCE is zero, which shows the environmental benefit of using PV to generate electricity. The system behavior for the period of 48hrs as shown in Fig. 11, revealed that, the output generated power from the PV is in multiple of the load demand; this was done to ensure the highest possible reliability and to reduce the impact of its intermittency on its reliability. Despite this, the system reliability was still not up to 100%.

### Case 3: EVO-optimized HPS

The optimal configuration of the solar PV, Battery, and DG using EVO is considered as Case3. The battery was used to store the excessive energy generated by the PV during the peak production hours and then to supply the load when the power generation from the solar PV is minimal. In this case, DG was used as a backup to provide the load that the solar PV and the battery do not meet. The optimal sizing of PV modules, Battery units, and DG that minimized NPC, LCOE, and TCE and maximized the SR was determined using EVO. The results are presented in Table 1. For this case, 208 modules of 500watt panels and 45 units of 250AH

battery are required with a DG rating of 22kW to supply the load demand of the proposed community. The NPC of the system for 20 years of operation is \$ 326000, while the cost of electricity per kWhr is 0.4889. The system with 100% reliability was realized using the proposed EVO-optimized HPS. The total CO<sub>2</sub> emission for 20 years is 775958.15 kg, equivalent to 4.43 kg of CO<sub>2</sub> per hour. The system behavior for 48 hours as presented in Fig. 12 shows that the battery was used to supply the load demand from 1 am to 7 am before the PV power production began. The State of Charge (SOC) of the battery decreased during this period from 100% to around 55% and started increasing when the generated power from the PV was above the load demand. This process describes the charging and discharging of battery storage used. DG was used (around 8 pm) when the battery SOC was closed to a minimum, and its available power was below the load demand. The coordinated operation of an optimized HPS compensated for the intermittency of the renewable energy source (solar PV) and enhanced 100% reliability. The convergence characteristics of the proposed EVO were examined, and the result presented in Fig. 13 revealed that EVO has a good convergence characteristic as its solution converged at the 8<sup>th</sup> iteration.

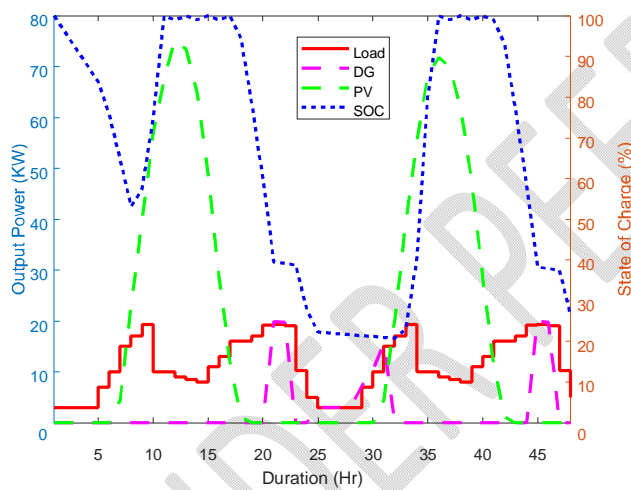


Fig. 12: System Behavior for 48hrs for Case 3

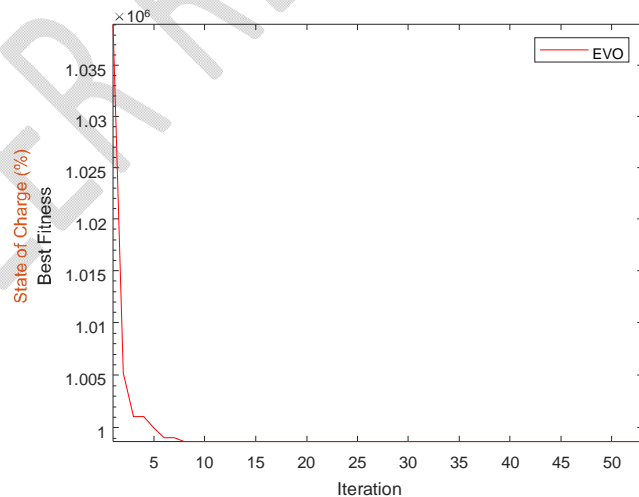


Fig. 13: Convergence Curve of the EVO

### Comparison of all the Cases Considered

All the cases considered were compared in terms of NPC, LCOE, TCE, and SR, and the results are presented in Fig. 14. It can be observed from Fig. 14 that the NPC for Case 1 is the highest, followed by that of Case 2, while Case 3 gave the lowest NPC. The LCOE of Case 1 is the highest, while the one for Case 3 is the lowest. The implication is that the proposed EVO-optimized HPS proffers economic benefits; it reduces the NPC and LCOE of the system, making the electricity more affordable to the user. While comparing the TCE of the cases considered, it

was observed that Case 1 had a detrimental effect on the environment as it gave the highest carbon emission. Case 2 proffered zero-emission, making it the best clean energy source for TCE. A remarkable reduction in TCE was recorded when Case 1 and Case 3 were compared; this implies that applying the proposed HPS can reduce the TCE and provide a safe environment. Regarding the system reliability, Case 1 and Case 3 had 100% reliability with zero LPSP, while Case 2 had 91.79% reliability with an LPSP of 0.0821.

### HOMER Optimized HPS

HOMER is a simulation software developed by the Energy Department of the United States of America (USA). It is a standard simulation tool to optimize hybrid power systems. HOMER software was also used to optimize the sizing of PV, battery, and DG, resulting in the formulation of HOMER-optimized HPS. The simulation results for HOMER-optimized HPS are presented in Table 2. As presented in Table 2, 174 modules of 500watt solar PV panels and 45 units of 250AH battery are required with a DG rating of 22kW to supply the load demand of the proposed community. The NPC of the system for 20 years is \$ 1011984.27, while the cost per kWhr of electricity using this system is 0.4957. The TCE of the system was recorded to be 832912.49 kg, while the LPSP of the system is zero (0), signifying 100% reliability. The system performance for 48hrs is presented in Fig. 15.

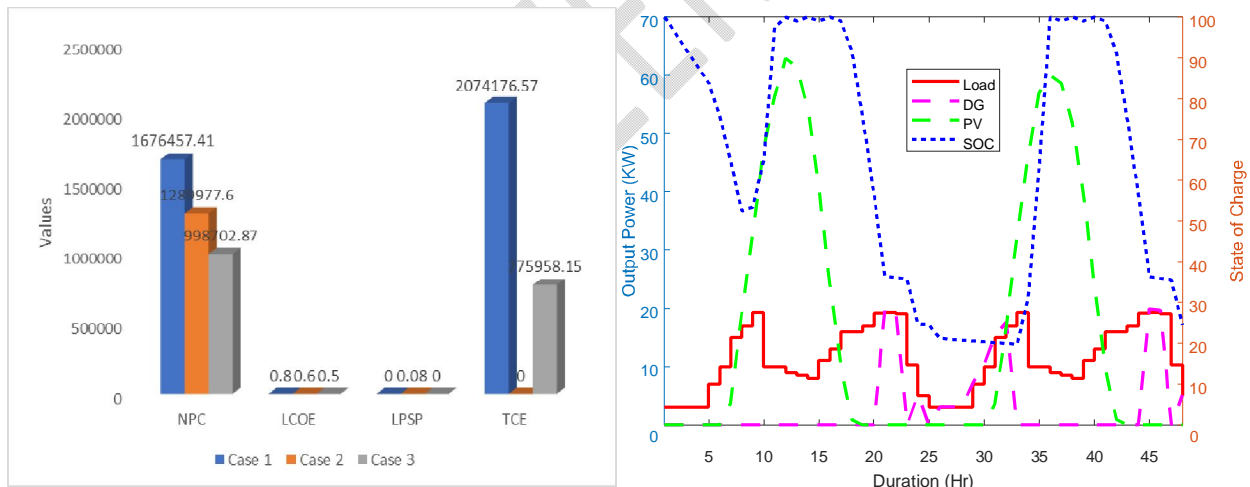


Fig. 14: Comparison of all the Cases Considered Fig. 15: System Behavior of HOMER-HPS

### Comparison of EVO-Optimized HPS and HOMER-Optimized HPS

HOMER software was used to compare the performance of the developed EVO-optimized HPS to validate its performance. Fig. 16 and 17 present the comparison of HOMER-optimized HPS and EVO-optimized HPS in terms of capital cost, operation and maintenance cost, replacement cost, fuel cost, salvage cost, NPC, LCOE, Hour of operation of DG, TCE and LPSP. From Fig. 16, it can be observed that the capital cost, operation and maintenance cost, and salvage cost for

EVO-optimized HPS is higher than that of HOMER; however, the replacement cost, fuel cost, NPC and LCOE of EVO-optimized HPS is lower compare to that of HOMER. This shows that though the HOMER-optimized HPS in terms of cost benefits. Furthermore, from Fig. 17, it can be deduced that both the developed approach and HOMER had zero LPSP, but in terms of TCE, the developed approach gave the lowest TCE. The outcome of the overall comparison between the EVO and HOMER optimizer revealed that the optimizer used on HPS could either improve or deteriorate its performance.

Table 2: Simulation Result for HOMER-Optimized HPS

Parameter	Value
Number of PV Panel	174
Number of Battery Unit	45
DG rating	22.00Kw
Hour of operation of DG	83420
Capital Cost	\$ 283500.00
Replacement Cost	\$ 206946.61
Operation and Maintenance cost	\$ 112730.84
Fuel Cost	\$ 564194.52
Salvage cost	\$ 155387.70
NPC	\$ 1011984.27
LCOE	0.4954 \$/kWhr
LPSP	0.00
TCE	832912.49kg

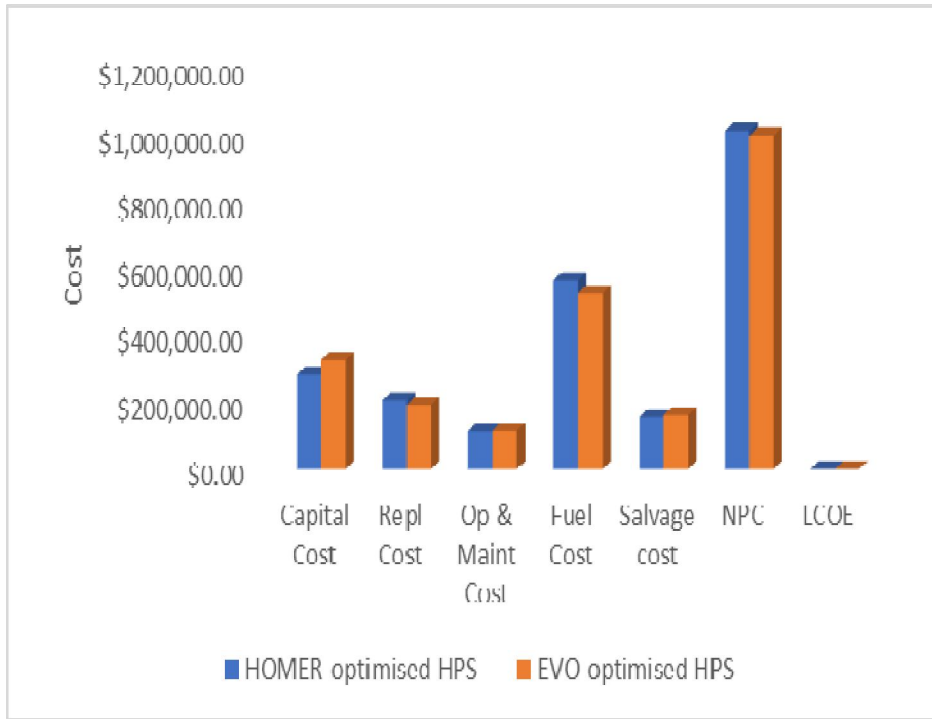


Fig. 16: Cost Comparison of HOMER-Optimized HPS and EVO-Optimized HPS

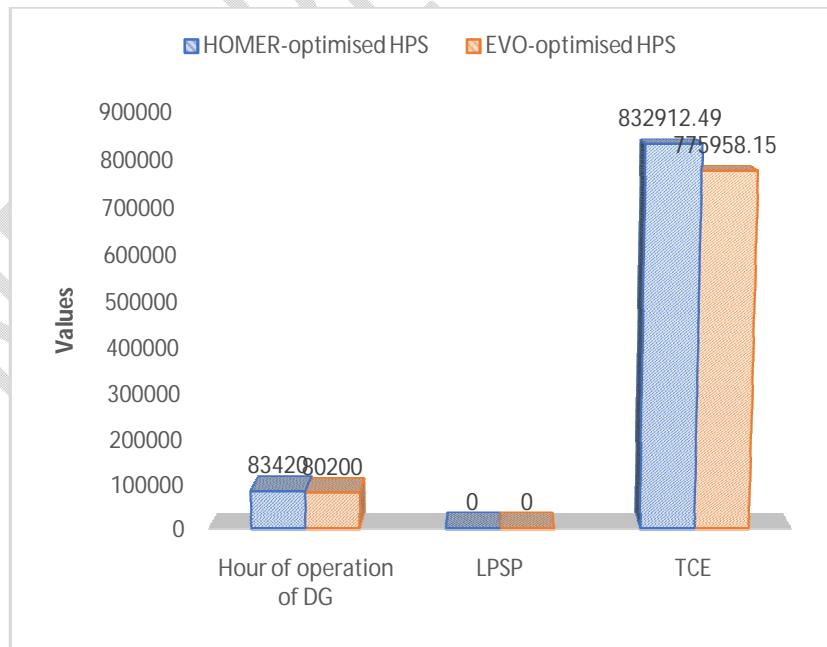


Fig. 17: Reliability and Emission Comparison

## Conclusion

In this work, an optimized Hybrid Power System (HPS) comprising PV, Battery, and DG is designed for rural electrification using Energy Valley Optimizer (EVO). The feasibility study was conducted on Ibudo-ora, a rural community in Surulere Local Government Area, Oyo state, to estimate the load demand of the community, and the resulting data such as load profile, solar irradiance, clearness index, and temperature were used in MATLAB simulation of the proposed design. A multi-objective function was developed to minimize the Net Present Cost (NPC), Levelized Cost of Electricity (LCOE), Total Carbon Emission, and Loss of Power Supply Probability (LPSP) of the developed HPS and optimize using EVO.

The simulation results revealed that the hybridization of different energy sources can reduce the cost of electricity, increase the system's reliability, and provide a safer way of generating electricity. Furthermore, the effect of the optimization approach used in optimizing the sizes of the components of the hybrid power system was demonstrated using EVO and HOMER Optimizer. The result revealed that the optimizer's effectiveness can limit the techno-economic benefits derived from HPS. The EVO optimizer realized an HPS with minimum cost, minimum emission, and high system reliability.

Therefore, EVO-based HPS can be used for rural electrification in the Ibudo-ora community to enhance technical, economic, and environmental benefits.

### Disclaimer (Artificial intelligence)

Author(s) hereby declare that NO generative AI technologies such as Large Language Models (ChatGPT, COPILOT, etc.) and text-to-image generators have been used during the writing or editing of this manuscript.

## References

- Askarzadeh, A., Dos, L. and Coelho, S. (2015). A novel framework for optimization of a grid independent hybrid renewable energy system: A case study of Iran. *Solar Energy* 112 (2015) 383–396. <http://dx.doi.org/10.1016/j.solener.2014.12.013>
- Azizi, M., Aickelin, U., Khorshidi, H. A. and Shishegarkhaneh, M. B. (2023). Energy valley optimizer: a novel metaheuristic algorithm for global and engineering optimization. *Scientific Reports*. (2023) 13:226. Pg 1-23. <https://doi.org/10.1038/s41598-022-27344-y>
- Babatunde, O. M., Denwigwe, I. H., Babatunde, D. E., Ayeni, A. O., Adedaja, T. B. and Adedaja, O. S. (2019). Techno-economic assessment of photovoltaic-diesel generator-battery energy system for base transceiver stations loads in Nigeria, *Cogent Engineering*, 6:1, 1684805, DOI: 10.1080/23311916.2019.1684805

- Babatunde, O., Buraimoh, E., Tinuoye, O., Ayegbusi, C., Davidson, I. and Ighravwe, D. E. (2023). Electricity sector assessment in Nigeria: the post-liberation era, *Cogent Engineering*, 10: 2157536 pg 1-14. <https://doi.org/10.1080/23311916.2022.2157536>
- Baghdadi, F., Mohammedi, K., Diaf, S. and Behar, O. (2015) Feasibility study and energy conversion analysis of stand-alone hybrid renewable energy system. *Energy Conversion and Management*. **105**(2015):471–479. <http://dx.doi.org/10.1016/j.enconman.2015.07.051>
- Chauhan, A and Saini, R. P. (2016). Discrete harmony search-based size optimization of Integrated Renewable Energy System for remote rural areas of Uttarakhand state in India. *Renewable Energy* 94 (2016) 587-604. <http://dx.doi.org/10.1016/j.renene.2016.03.079>
- Fadaeenejad, M., Radzi, M.A.M., AbKadir, M.Z.A. and Hizam, H. (2014) Assessment of hybrid renewable power sources for rural electrification in Malaysia. *Renewable and Sustainable Energy Reviews* 30 (2014) 299–305. <http://dx.doi.org/10.1016/j.rser.2013.10.003>
- Hoarcă, I. C., Bizon, N., Șorlei, I. S. and Thounthong, P. (2023). Sizing Design for a Hybrid Renewable Power System Using HOMER and iHOGA Simulators. *Energies*. 2023; 16(4):1926. Pg 1-26. <https://doi.org/10.3390/en16041926>
- Jumare, I. A., Bhandari, R. and Zerga, A. (2020). Assessment of a decentralized gridconnected photovoltaic (PV) / wind/ biogas hybrid power system in norther Nigeria. *Energy, Sustainability and Society* (2020) 10:30 Page 2-25. <https://doi.org/10.1186/s13705-020-00260-7>
- Kabira, E., Kumar, P., Kumar, S., Adelodun, A. A. and Kim, K. (2018). Solar energy: Potential and future prospects *Renewable and Sustainable Energy Reviews* 82 (2018): 894–900
- Kamal, M. M., Mohammad, A., Ashraf, A. and Fernandez, E. (2022). Rural electrification using renewable energy resources and its environmental impact assessment. *Environmental Science and Pollution Research* (2022) 29:86562–86579 <https://doi.org/10.1007/s11356-022-22001-3>
- Kharrich, M., Mohammed, O. H., Alshammari, N., and Akherraz, M. (2021). Multi-objective optimization and the effect of the economic factors on the design of the microgrid hybrid system. *Sustainable Cities and Society*, 65, 102646.
- Krishan, O. and Suhag, S. (2019). Techno-economic analysis of a hybrid renewable energy system for an energy poor rural community. *Journal of Energy Storage* 23 (2019) 305–319. <https://doi.org/10.1016/j.est.2019.04.002>
- Mahmud, S., Kaihan, M. K., Salehin, S., Ferdaous, M. T. and Nasim, M. (2022). Hybrid renewable energy systems for a remote community in a high mountain plateau. *International Journal of Energy and Environmental Engineering* (2022) 13:1335–1348 <https://doi.org/10.1007/s40095-022-00494-5>
- Mojumder, M. F. H., Islam, T., Chowdhury, P., Hasan, M., Takia, N. A., & Farrok, O. (2024). Techno-economic and environmental analysis of hybrid energy systems for remote areas: A sustainable case study in Bangladesh. *Energy Conversion and Management: X*, 23, 100664, pg 1-28.
- Movahediyani, Z. and Askarzadeh, A. (2018). Multi-objective optimization framework of a photovoltaic-diesel generator hybrid energy system considering operating reserve. *Sustainable Cities and Society* 41 (2018) 1–12.
- National Aeronautic and Space Administration (2023): <https://power.larc.nasa.gov>
- Nazari-Heris M. and Mohammadi-Ivatloo B. (2018). *Classical and Recent Aspects of Power System Optimization*. Elsevier Inc. All rights reserved. ISBN 978-0-12-812441-3. <https://doi.org/10.1016/B978-0-12-812441-3.00002-1>.

- Ogunjuigbe, A.S.O. and Ayodele, T.R. (2016). Techno-economic analysis of stand-alone hybrid energy system for Nigerian telecom industry. *Int. J. Renewable Energy Technology*, Vol. 7, No. 2, pp.148–162.
- Ogunjuigbe, A.S.O., Ayodele, T.R. and Akinola, O.A. (2016). Optimal allocation and sizing of PV/Wind/Split-diesel/Battery hybrid energy system for minimizing life cycle cost, carbon emission and dump energy of remote residential building. *Applied Energy* 171 (2016) 153–171  
<http://dx.doi.org/10.1016/j.apenergy.2016.03.051>
- Qi, X., Wang J, Krolczyk, G., Gardoni, P. and Li. Z. (2022). Sustainability analysis of a hybrid renewable power system with battery storage for islands application. *Journal of Energy Storage*. 50 (2022): 1-12.<https://doi.org/10.1016/j.est.2022.104682>
- Saputra, A., Setyawan, A., Chairiman, C., Putri, A. I., & Diguna, L. J. (2024). Techno-economic analysis of hybrid PV-Battery-diesel system for isolated Dockyard in West Papua. In *E3S Web of Conferences* (Vol. 475, p. 03008). Pg 1-12. EDP Sciences.
- Sawle, Y., Gupta, S. C. and Bohre, A. K. (2018). Review of hybrid renewable energy systems with comparative analysis of off-grid hybrid system. *Renewable and Sustainable Energy Reviews* 81 (2018) 2217–2235. <http://dx.doi.org/10.1016/j.rser.2017.06.033>
- Sinha, S. and Chandel, S. (2014). Review of software tools for hybrid renewable energy systems. *Renewable and Sustainable Energy Reviews*. Elsevier Ltd. 32 (2014):192–205  
<http://dx.doi.org/10.1016/j.rser.2014.01.035>
- Suresh, V., Muralidhar, M. and Kiranmayi, R. (2020). Modelling and optimization of an off-grid system for electrification in a rural area. *Energy Reports*. 6(2020):594–604.  
<https://doi.org/10.1016/j.egy.2020.01.013>
- The World Bank (2023, May). World Development Indicators, Access to electricity (% of population), from World bank data: <https://data.worldbank.org/indicator/EG.ELC.ACCS.RU.ZS>
- Tito, S.R., Lie, T.T. and Anderson, T.N. (2016). Optimal sizing of a wind-photovoltaic-battery hybrid renewable energy system considering socio-demographic factors. *Solar Energy* 136 (2016) 525–532.<http://dx.doi.org/10.1016/j.solener.2016.07.036>
- Yahiaouia, A., Fodhilb, A., Benmansoura, K., Tadjinec, M. and Cheggagab, N. (2017). Grey wolf optimizer for optimal design of hybrid renewable energy system PV-Diesel Generator-Battery: Application to the case of Djanet city of Algeria. *Solar Energy*. 158(2017):941–951.<http://dx.doi.org/10.1016/j.solener.2017.10.040>